

An Antibody Blocking Activin Type II Receptors Induces Strong Skeletal Muscle Hypertrophy and Protects from Atrophy

Estelle Lach-Trifilieff,^a Giulia C. Minetti,^a KellyAnn Sheppard,^c Chikwendu Ibebunjo,^b Jerome N. Feige,^{a*} Steffen Hartmann,^d Sophie Brachat,^a Helene Rivet,^a Claudia Koelbing,^a Frederic Morvan,^a Shinji Hatakeyama,^a David J. Glass^b

MusculoSkeletal Diseases, Novartis Institutes for Biomedical Research, Basel, Switzerland^a; MusculoSkeletal Diseases, Novartis Institutes for Biomedical Research, Cambridge, Massachusetts, USA^b; Development and Molecular Pathways, Novartis Institutes for Biomedical Research, Cambridge, Massachusetts, USA^c; Integrated Biologics Profiling, Novartis Pharma, Basel, Switzerland^d

The myostatin/activin type II receptor (ActRII) pathway has been identified to be critical in regulating skeletal muscle size. Several other ligands, including GDF11 and the activins, signal through this pathway, suggesting that the ActRII receptors are major regulatory nodes in the regulation of muscle mass. We have developed a novel, human anti-ActRII antibody (bimagrumab, or BYM338) to prevent binding of ligands to the receptors and thus inhibit downstream signaling. BYM338 enhances differentiation of primary human skeletal myoblasts and counteracts the inhibition of differentiation induced by myostatin or activin A. BYM338 prevents myostatin- or activin A-induced atrophy through inhibition of Smad2/3 phosphorylation, thus sparing the myosin heavy chain from degradation. BYM338 dramatically increases skeletal muscle mass in mice, beyond sole inhibition of myostatin, detected by comparing the antibody with a myostatin inhibitor. A mouse version of the antibody induces enhanced muscle hypertrophy in myostatin mutant mice, further confirming a beneficial effect on muscle growth beyond myostatin inhibition alone through blockade of ActRII ligands. BYM338 protects muscles from glucocorticoid-induced atrophy and weakness via prevention of muscle and tetanic force losses. These data highlight the compelling therapeutic potential of BYM338 for the treatment of skeletal muscle atrophy and weakness in multiple settings.

Skeletal muscle wasting occurs in a variety of pathophysiological settings, including sepsis, renal failure, diabetes, chronic obstructive pulmonary disease (COPD), and cancer. Furthermore, muscle atrophy arises after injury because of muscle inactivity resulting from casting, immobilization, or prolonged bed rest (1) and also as a result of the age-related loss of skeletal muscle known as sarcopenia, which is part of the broader syndrome of frailty often observed in elderly individuals (2, 3). Extensive studies have documented the key role of myostatin as a negative regulator of skeletal muscle mass, acting primarily via the activin type IIB receptor (ActRIIB) (4). After myostatin's discovery (5), there were numerous subsequent observations that myostatin loss-of-function mutations in a range of species, including cattle, sheep, dogs, and humans, all resulted in a significant increase in muscle mass (6–9). In addition to myostatin (5, 6), other negative regulators of muscle mass have been reported to signal through ActRIIB, including activin A (10–13), while some uncertainty with regard to the contribution of the closely related GDF11 at regulating muscle mass and function remains (13–15). However, a broad survey of transforming growth factor β (TGF- β) ligands that were capable of blocking muscle differentiation and inducing muscle fiber atrophy included GDF11, activins A and B, and TGF- β itself (16).

Myostatin, GDF11, and activins (A and B) bind to and signal through either the ActRIIA or ActRIIB receptor on the cell membrane, with ActRIIB initially identified to be myostatin's prime receptor (13, 17, 18). Upon binding to ActRII, the ligand and type II receptor form a complex with a type I receptor, either activin receptor-like kinase 4 (ALK4) or ALK5, to stimulate the phosphorylation of the Smad2 and Smad3 transcription factors in the cytoplasm. Phosphorylated Smad2/3 are then translocated to the nucleus and modulate the transcription of target genes, including MyoD (4, 16).

Myostatin's inhibition of muscle differentiation and hypertrophy has been reported to occur at least partially through a Smad2/3 phosphorylation-dependent blockade of the AKT-mTOR pathway; treatment of muscle with myostatin or activin results in a decrease in the level of phosphorylated AKT (16, 19), which is required for muscle differentiation in the myoblast (19) and which mediates muscle hypertrophy in the myofiber (20). However, in the absence of AKT isoforms, i.e., in AKT1- and AKT2-knockout mice, ActRIIB inhibition, likely via myostatin and activin blockade, could still increase muscle size and function (21), indicating that there are non-AKT-mediated components of the overall myostatin response.

In addition to myostatin, there are other TGF- β family members induced in muscle by inflammatory cytokines. In particular, activin A has been found to be upregulated in skeletal muscle after activation of the tumor necrosis factor α /TAK-1 signaling pathway (12). Furthermore, inhibition of activin A in this model is sufficient to block atrophy. This finding demonstrates that, similar to the case of individual cytokines, blocking individual TGF- β family members such as myostatin alone may not be sufficient in

Received 1 October 2013 Returned for modification 21 October 2013

Accepted 18 November 2013

Published ahead of print 2 December 2013

Address correspondence to Estelle Lach-Trifilieff, estelle.trifilieff@novartis.com, or David J. Glass, david.glass@novartis.com.

* Present address: Jerome N. Feige, Institute of Health Sciences, EPFL, Lausanne, Switzerland.

Copyright © 2014, American Society for Microbiology. All Rights Reserved.

doi:10.1128/MCB.01307-13

The authors have paid a fee to allow immediate free access to this article.

settings such as cancer cachexia. Many human cancers present with altered expression of activin A, associated with a more malignant phenotype (22, 23), and tumors can also induce the release of activin A from muscle (12). Intervention at the ActRIIB pathway level under cancer cachexia conditions in mice showed a clear benefit not only for muscle preservation but also for overall survival, without affecting tumor growth (24).

Mice engineered to overexpress either the myostatin propeptide (which inhibits only myostatin signaling), the naturally occurring myostatin and activin inhibitor follistatin, or a dominant negative form of the ActRIIB all led to mice display increases in muscle mass even greater than those observed in the myostatin mutant (18).

Multiple myostatin pathway pharmacological inhibitors have recently been generated, given the therapeutic potential of stimulating muscle growth or preventing muscle loss in settings of human disease. These include neutralizing antibodies to myostatin (25), a modified myostatin propeptide which blocks myostatin (26), and a soluble ActRIIB-Fc receptor trap (10, 21, 24, 27), all of which increase postnatal muscle growth in mice. Administration of soluble ActRIIB led to muscle hypertrophy in normal and myostatin-knockout mice, suggesting that other ligands, in addition to myostatin, normally function to limit muscle growth (10). Thus, the capacity for modulating muscle growth by perturbing this signaling pathway at the receptor level is much greater than that achieved by blocking myostatin only. Given these prior data, it seemed possible that blockade of ActRII through a direct neutralizing antibody approach would significantly reduce the activity of myostatin and other ligands that inhibit skeletal muscle growth by signaling through these receptors. Evidence for the therapeutic potential of this approach for the treatment of multiple conditions associated with muscle wasting is presented here.

MATERIALS AND METHODS

Material and reagents. All of the proteins described here were produced at Novartis Pharma AG (Basel, Switzerland). These included myostatin propeptide D76A, ActRIIB-amyloid precursor protein (ActRIIB-APP), ActRIIA-APP (bimagrumab, or BYM338), an anti-ActRII antibody, and CDD866, a murinized version of BYM338, where the human Fc region of the antibody has been replaced by a mouse Fc. Fiber type I, IIa, and IIb rabbit polyclonal antibodies were kindly provided by the Novartis Biologic Units. Recombinant proteins, GDF8, and activin A were from R&D Systems. The fiber type IIx (BF35) rabbit polyclonal antibody was from the Developmental Studies Hybridoma Bank (DSHB). Dexamethasone 21-phosphate disodium salt was from Sigma-Aldrich. The following were used: anti-myosin heavy chain (anti-MyHC; Upstate Biotechnology); Alexa Fluor 488-F(ab'), Alexa Fluor 565, Alexa Fluor 350, Alexa Fluor 488, and Alexa Fluor 555 (Invitrogen); phospho-Smad2 (Ser465/467), phospho-Smad3 (Ser423/425), phospho-AKT (Ser473), total Smad2, total AKT, and antidesmin (Cell Signaling Technology); anti-myosin (skeletal, fast and slow) and anti- α -tubulin (Sigma-Aldrich); anti-myogenin F5D (BD Biosciences); GAPDH (glyceraldehyde-3-phosphate dehydrogenase; Life Technologies); and rabbit polyclonal antibody against laminin (Sigma).

SET. Solution equilibrium titration (SET) experiments were performed as described by Haenel et al. (28); however, a plate-based assay setup was used for detection. In brief, dilution series of monomeric antigens were prepared, and BYM338 was added at a constant antibody concentration. After overnight incubation, the antibody-antigen preparation was transferred into an antigen-coated High Bind microtiter plate (Meso Scale Discovery) for 25 min. After washing, electrochemiluminescence detection was achieved with 25 μ l of 1 μ g/ml sulfo-Tag-labeled goat anti-

human detection antibody (MesoScale Discovery) and 50 μ l of read buffer (MesoScale Discovery) per well using a Sector Imager 6000 reader (MesoScale Discovery).

Cell lines and treatments. Adult human skeletal muscle cells (from 50- and 51-year-old donors) (Cook Myosite, Pittsburgh, PA) were cultured in growth medium consisting of myotonic basal medium supplemented with myotonic growth supplement (Cook Myosite), 20% fetal calf serum (FCS; PAA Laboratories), 10 μ g/ml insulin (Amimed Direct Ltd., United Kingdom), and 0.1% gentamicin (Life Technologies Ltd., Paisley, United Kingdom). For differentiation experiments, cells were seeded on collagen I (Gibco, Life Technologies Ltd., United Kingdom). Differentiation was initiated 24 h after seeding by changing to differentiation medium consisting of myotonic differentiation medium supplemented with 2% horse serum (PAA Laboratories), 1% FCS, 0.1% gentamicin. Cells were starved for at least 4 h in myotonic differentiation medium supplemented with 0.05% bovine serum albumin (BSA; Sigma-Aldrich), before treatment. Fetal human skeletal muscle cells (7F, 11F; Lonza) were cultured on Matrigel matrix (BD Biosciences) in growth medium consisting of skeletal muscle basal medium (skBM; Lonza) supplemented with 20% FCS. Differentiation was initiated 24 h after seeding by changing to serum-free medium consisting of skBM plus 0.5% gentamicin (Invitrogen). Cells were stimulated with myostatin or activin A alone or in the presence of BYM338 during the necessary time according to the assay.

Reporter gene assay. The Smad2/3 response was evaluated in a CAGA12-luciferase reporter assay using HEK293T cells stably transfected with pGL3-CAGA12-Luc. Cells were seeded in serum-reduced medium (2% FCS) for 24 h, prior to cell stimulation with myostatin or activin A alone or in the presence of BYM338 for another 24 h. Luciferase activity was measured using Britelite Plus reagent (PerkinElmer).

CK activity assay. A creatine kinase (CK) activity assay was performed as described previously (12).

Immunostaining and myotube size analysis. To analyze changes in myotube size, differentiating myoblasts or differentiated myotubes were washed with cytoskeleton stabilizing buffer (CSB) consisting of 80 mM PIPES [piperazine-*N,N'*-bis(2-ethanesulfonic acid)], 5 mM EGTA, 1 mM MgCl₂, polyethylene glycol 35000 (40 g/liter) in distilled water (pH 7.4) and fixed with 4% paraformaldehyde in CSB for 15 min at room temperature. Cells were then permeabilized with 0.2% Triton in CSB, and non-specific binding was blocked with 10% normal goat serum (Zymed), followed by incubation with anti-MyHC antibody diluted in phosphate-buffered saline (PBS), 1.5% goat serum, and, subsequently, Alexa Fluor 488 diluted in PBS supplemented with DAPI (4',6-diamidino-2-phenylindole) solution (Promokine; Promocell, Heidelberg, Germany). The diameter of the myotubes from the entire well was measured using the Cell Insight technology. Data are expressed as the mean width compared to that for the control. A fusion index was calculated as the average number of nuclei per myotube. A differentiation index was calculated as the percentage of nuclei in MyHC-positive cells relative to the total number of nuclei.

Phosphorylation analysis using the AlphaScreen SureFire protocol for P-Smad3. Samples were prepared with PhosphoSafe lysis buffer as described below in "Immunoblotting." The AlphaScreen SureFire protocol for phosphorylated Smad3 (P-Smad3; P-Ser423/425) was performed according to the manufacturer's instructions in a 384 ProxiPlate. The signal was read using a SpectraMax Paradigm absorbance detection cartridge (Molecular Devices, Sunnyvale, CA) with an AlphaScreen cartridge.

Phosphorylation analysis using a Meso Scale Discovery kit for P-AKT. Quantitative determination of phosphorylated AKT (P-AKT; Ser473) in whole-cell lysate was performed using an AKT Signaling Panel II whole-cell lysate kit (K15177D-1) and normalized on an AKT Signaling Panel II base kit (K12177A-3) from MesoScale Discovery using a MesoScale Discovery reader according to the manufacturer's instruction.

Immunoblotting. Cells were lysed with PhosphoSafe lysis buffer (Novagen Inc., Madison, WI) supplemented with protease inhibitor cocktail

(Calbiochem, Merck, Millipore, Germany) for Smad and AKT or with radioimmunoprecipitation assay buffer (Pierce; Rockford, IL) supplemented with 1% Halt protease (Thermo Fisher Scientific Inc., Waltham, MA) and 1% phosphatase inhibitor cocktail (Calbiochem) for MyHC and myogenin. Briefly, homogenates were separated by centrifugation for 15 min at 4°C (14,000 rpm). Supernatants were collected, and protein contents were measured with a bicinchoninic acid kit (Pierce). Samples were solubilized in SDS-PAGE sample buffer supplemented with beta-mercaptoethanol (Sigma-Aldrich). Equal amounts of protein were loaded per lane. For Smad, AKT, and myogenin analysis, samples were loaded in a 4 to 12% polyacrylamide gel (NuPAGE bis-Tris gel; Invitrogen) and transferred onto nitrocellulose membranes (Invitrogen) using a Semi-Dry I blot system (Invitrogen). For MyHC fast and slow analysis, the samples were loaded in a 3 to 8% Tris-acetate gel (Invitrogen) and transferred onto polyvinylidene difluoride membranes (Invitrogen) using a wet transfer system (Invitrogen) in the presence of 10% methanol (Sigma-Aldrich). Membranes were blocked in Tris-buffered saline (TBS) with 5% milk powder. Primary and secondary antibodies were incubated in TBS with 0.1% Tween 20 and 5% milk or 5% BSA. Immunoreactivity was detected by chemiluminescence using SuperSignal West Femto maximum-sensitivity substrate (ThermoFisher), the ECL Plus reagent (Amersham), or the ECL reagent (Amersham) and exposed to film.

RNA isolation from muscle samples and analysis. RNA was isolated from the mouse tibialis muscle with a TRIzol Fast Prep kit (Invitrogen), according to the manufacturer's instructions. cDNA synthesis was performed with a high-capacity cDNA reverse transcription kit (Applied Biosystems). Real-time PCR was performed with an Applied Biosystems 7500 Fast PCR machine. The TaqMan probe sets for muscle RING finger 1 (MuRF1; Mm01185221_m1), muscle atrophy F box (MAFbx; Mm00499518_m1), and GAPDH (Mm4352339E) were purchased from Applied Biosystems.

Animal efficacy studies. (i) BYM338 in naive mice. Animal experiments were performed in accordance with the Swiss ordinance on animal experimentation after approval by cantonal veterinarian authorities under license number BS-2127. Ten-week-old C57BL/6J-Crj (SCID) female mice were obtained from Charles River, Germany, and maintained in a 12-hour light–12-hour dark cycle with unrestricted access to a regular diet containing 18.2% protein and 3.0% fat with an energy content of 15.8 MJ/kg (NAFAG 3890; Klüber-Nafag, Basel, Switzerland) and water. After 7 days of acclimation in the facility, the mice were randomized to treatment groups by body weight before starting the experiment and treated once weekly with BYM338 at 6 mg/kg of body weight or 20 mg/kg subcutaneously (s.c.). Body weights were determined once weekly. After 4 weeks, the mice were euthanized with CO₂. Serum was collected, and the tibialis anterior muscle and the gastrocnemius muscle with the plantaris, soleus, and extensor digitorum longus (EDL) muscles were collected and weighed. RNA samples were extracted from the gastrocnemius muscle of mice after 4 weeks of treatment with BYM338 at 20 mg/kg or vehicle ($n = 8$). In a following experiment comparing BYM338 at 10 mg/kg to myostatin propeptide D76A at 30 mg/kg, the SCID mice were treated once weekly for 5 weeks, with an additional administration on day 3.

(ii) Chimeric BYM338 in myostatin-deficient mice. Adult male homozygous C57BL/6J-Mstnlean/J mice (referred to as Mstn^{Ln/Ln} mice) 15 to 20 weeks of age were purchased from The Jackson Laboratory (stock 009345). Age-matched male C57BL/6J mice were purchased from Charles River Laboratories. Mice were housed at three per cage in a temperature- and humidity-controlled environment with 12-h light–12-h dark cycles and free access to standard rodent chow (Klüber-Nafag, Kaiseraugst, Switzerland) and tap water. Animals were acclimatized to their housing conditions for 4 weeks and randomized to treated and untreated groups according to body weight and lean mass. Wild-type (wt) mice ($n = 10$ /group) and Mstn^{Ln/Ln} mice ($n = 8$ /group) were treated with a subcutaneous injection of PBS or CDD866 (murinized BYM338) at 20 mg/kg on days 0, 7, 14, 21, and 28. Body weight was measured weekly, and fat and lean masses were measured

on day 0 and day 21 using a mouse body composition nuclear magnetic resonance (NMR) analyzer (Minispec LF50; Bruker Optics, Germany).

(iii) BYM338 in mouse glucocorticoid-induced myopathy model. Adult 4-month-old male C57BL/6 mice were purchased from Taconic Laboratories and acclimated to the facility for at least 7 days. They were randomized by body weight into groups of 10 mice each, housed at 2 mice per cage in a temperature-controlled (72°F) and humidity-controlled (43%) room, and maintained on a 12-h light–12-h dark cycle. All mice were fed a standard rodent diet (5053, PicoLab Rodent Diet 20; LabDiet). Food and water were provided *ad libitum*. This study was performed according to protocol 08 MG 0274, approved by the Novartis Institutes for Biomedical Research (NIBR) Institutional Animal Care and Use Committee. All procedures used in the study were in compliance with Animal Welfare Act Regulations 9 CFR Parts 1, 2, and 3 and U.S. regulations (29). For glucocorticoid-induced skeletal muscle atrophy and weakness, dexamethasone (DEX) was administered to mice via the drinking water at a dose of 2.4 mg/kg/day. To evaluate whether BYM338 prevents DEX-induced myopathy, BYM338 was administered at 5 or 20 mg/kg/week subcutaneously during the 14 days of DEX administration. To evaluate whether BYM338 facilitates muscle recovery after DEX-induced myopathy, mice were administered DEX at ~2.4 mg/kg/day for the first 21 days and administered BYM338 at 5 and 20 mg/kg or the IgG1-LALA isotype at 20 mg/kg intraperitoneally (i.p.) on days 21, 23, and 28. Mice that did not receive DEX in water served as experimental controls. Because administration of DEX caused an increase in drinking, the concentration of DEX was adjusted periodically, whenever water intake changed by 2 ml/day, in order to maintain the dose at 2.4 mg/kg/day. At the end of the experiment, peak nerve-evoked tibialis muscle force was assessed using a muscle physiology system (Aurora Scientific, Inc., Aurora, Ontario, Canada) as described previously (30) but with the baseline tension on the tibialis muscle set at ~5 g, which yielded the peak evoked force. The peak force generated during stimulation at 240 Hz was measured as the peak tetanic force. After assessment of evoked muscle strength, euthanasia was performed by CO₂ asphyxiation, blood was collected by cardiac puncture to obtain serum, and skeletal muscle from the hind legs (tibialis anterior, gastrocnemius-soleus-plantaris complex, and quadriceps muscles) and heart, liver, spleen, and perirenal white adipose tissues were rapidly dissected out and weighed. The right tibialis anterior muscle was snap-frozen in 2-methylbutane precooled in liquid nitrogen for histological analysis, while all other muscles and tissues were snap-frozen directly in liquid nitrogen and stored at –80°C. Alternatively, the tibialis muscle was dissected, fixed in 10% buffered formalin or embedded in OCT specimen matrix compound (Tissue-Tek), and frozen in cooled isopentane for histology analysis. Specimens embedded in paraffin were processed by the conventional hematoxylin-eosin method.

Fiber cross-sectional area analysis. Ten-micrometer-thick serial sections of the frozen gastrocnemius muscle with plantaris were cut in a cryostat. For immunohistochemical detection of laminin to outline the sarcolemma, cryosections were permeabilized with 0.5% Triton X-100 and blocked in 2% goat serum. Sections were incubated for 5 min in 5% H₂O₂ and then with rabbit polyclonal antibody to laminin and monoclonal antibody against type I (1:100) or type IIa (1:200), type IIb (1:100), or type IIx (1:500) fiber overnight at 4°C. After washing in PBS three times for 10 min each time, sections were incubated with Alexa Fluor 488 anti-rabbit secondary antibody (1:100; Invitrogen) for 1 h at 25°C, followed by three washes in PBS to detect laminin. Sections were then incubated with secondary antibody, Alexa Fluor 555, Alexa Fluor 350, Alexa Fluor 555, and Alexa Fluor 350 (all at 1:200 for 1 h at 25°C), to reveal type I, IIa, IIb, and IIx fibers, respectively, followed by three washes in PBS. Slides were mounted with ProLong Gold antifade reagent (Invitrogen). Images of the entire tissue section were acquired using an Olympus scan VS120 microscope (Olympus Corporation), and the cross-sectional area of the individual fibers in the section as well as their number was measured automatically using Robias Astoria (v.4.1) software. The means of the fiber

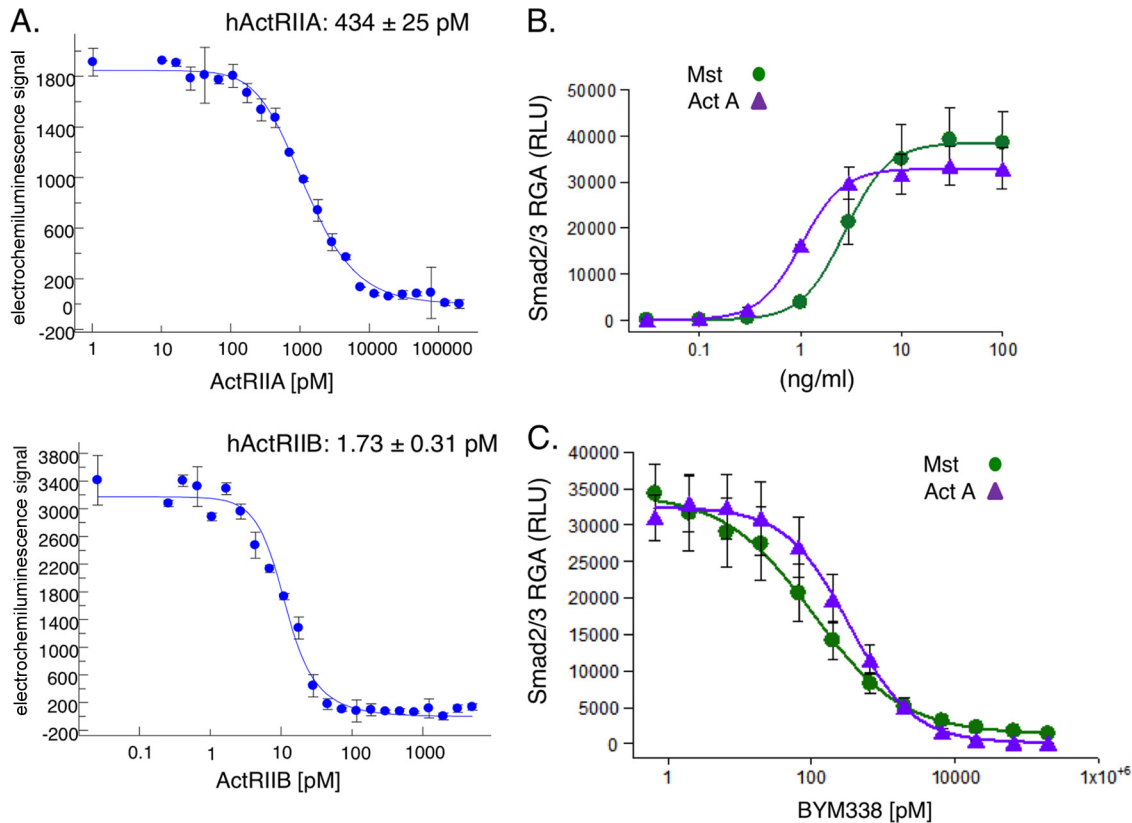


FIG 1 Affinity and potency of BYM338 at inhibiting myostatin (Mst) and activin A (Act A) signaling in a Smad2/3 CAG-luciferase reporter gene assay. (A) Affinity of BYM338 for human ActRIIA (hActRIIA) and human ActRIIB (hActRIIB) determined by solution equilibrium titration. Shown are representative examples of the results from 4 or 5 independent experiments. (B) Myostatin- and activin A-induced dose-dependent increases in Smad2/3 activity were measured with a CAGA-luciferase reporter stably expressed in HEK293 cells. (C) The ActRII-dependent response was determined upon addition of myostatin (10 ng/ml) or activin A (10 ng/ml) in the presence of increasing concentrations of BYM338. Shown are means \pm SEMs from 3 to 4 independent experiments. RGA, reporter gene assay; RLU, relative light units.

cross-sectional areas in each muscle section were determined, and the frequency distributions of the fiber cross-sectional area were plotted.

Gene expression profiling. RNA samples were extracted from the gastrocnemius muscle of mice after 4 weeks of treatment with either BYM338 at 20 mg/kg or vehicle ($n = 8$). These RNA samples were subjected to microarray analysis on Affymetrix GeneChip mouse genome 430 (v.2.0) chips (Affymetrix, Santa Clara, CA) according to the manufacturer's recommendations. All microarray statistical data analyses were performed as reported previously (31).

Statistical analysis. All results are presented as the mean \pm standard error of the mean (SEM) and were analyzed using one- or two-way analysis of variance (ANOVA) with the Dunnett or Bonferroni *post hoc* test or an unpaired two-tailed Student *t* test, according to the experimental design. Values were considered statistically significant at P values of <0.05 . Statistical analyses were performed by Prism software (GraphPad Software, Inc., La Jolla, CA). Muscle weight was normalized to the body weight at day 0 (initial body weight).

RESULTS

Binding properties and potency of BYM338. Bimagrumab (BYM338) is a fully human anti-ActRII antibody developed by MorphoSys AG (Munich, Germany) using its phage display technology. The affinity of BYM338 binding to human ActRIIA and ActRIIB was analyzed using solution equilibrium titration (Fig. 1A). After incubation of the antibody with serial dilutions of the respective antigen, an equilibrium dissociation constant (K_D) of 1.7 ± 0.3 pM was determined for human ActRIIB and a K_D of

434 ± 25 pM was determined for ActRIIA. Therefore, the antibody has a binding preference for ActRIIB of greater than 200-fold over that for ActRIIA, yet the affinity for ActRIIA is still in the subnanomolar range. Detailed kinetic information, obtained with surface plasmon resonance-based biosensor technology (Biacore T-100) with human ActRIIA and ActRIIB captured on the chip and the Fab of BYM338 as the analyte, corroborated the findings presented above, with a K_D of 4.62 ± 3.82 pM for human ActRIIB and a K_D of 490 ± 152 pM for human ActRIIA.

The potency of BYM338 for inhibition of signaling of ActRII ligands was assessed in a Smad2/3 CAGA-luciferase reporter gene assay in HEK293 cells (Fig. 1B). Both myostatin and activin A induced Smad2/3-dependent luciferase responses in a dose-dependent manner, with 50% effective concentrations (EC_{50} s) of 2.76 and 1.02 ng/ml, respectively (Fig. 1B). BYM338 inhibited myostatin-induced luciferase production with a 50% inhibitory concentration (IC_{50}) of 154 ± 73 pM (Fig. 1C). Similar dose-dependent inhibition of activin A-induced luciferase by BYM338 was observed, with an IC_{50} value of 343 ± 97 pM (Fig. 1C).

Promoting enhanced differentiation and hypertrophy of primary human skeletal muscle cells. The effects on myogenic differentiation were assessed upon treatment with BYM338 using primary human fetal or adult skeletal muscle cells. As shown in Fig. 2A, by myosin heavy chain (MyHC) staining, BYM338 increased differentiation and fusion 4 days after switching confluent

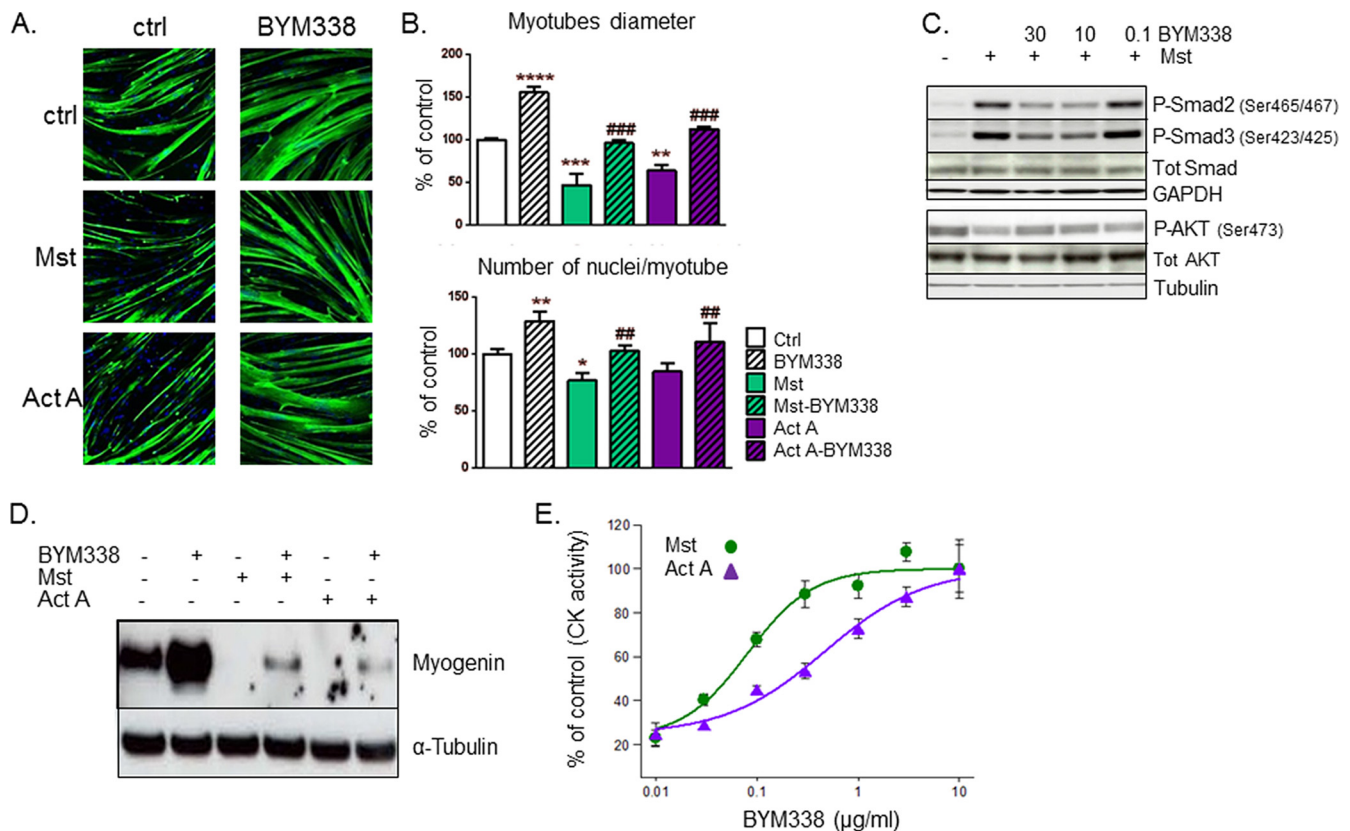


FIG 2 ActRII inhibition relieves myostatin and activin A inhibition of differentiation. (A) Human primary myoblasts differentiated for 4 days in the absence (control [ctrl]) and presence of myostatin (30 ng/ml) or activin A (30 ng/ml) alone and in combination with BYM338 (10 mg/ml) were stained for MyHC and with DAPI. Shown are representative pictures. (B) Analysis of myotube diameters and the fusion index performed as described in Materials and Methods. Data are expressed as a percentage of the values for the control. Shown are means \pm SEMs from 4 independent experiments. Asterisks indicate *P* values versus the control; pound signs indicate *P* values versus samples without BYM338 treatment. ****, *P* < 0.0001; *** or ###, *P* < 0.001; ** or ##, *P* < 0.01; *, *P* < 0.05. (C) BYM338 (mg/ml) reverses myostatin-induced Smad2/3 phosphorylation after 1 h of stimulation (myostatin was used at 10 ng/ml). At 24 h poststimulation, BYM338 prevents a reduction in AKT phosphorylation resulting from myostatin stimulation. Shown are representative immunoblots. Tot, total. (D) Immunoblotting of myogenin versus tubulin (as a loading control) from human primary myoblasts differentiated for 2 or 3 days in the absence or presence of myostatin (30 ng/ml) or activin A (30 ng/ml) alone and in combination with BYM338 (10 mg/ml). (E) Analysis of creatine kinase (CK) activity from myotubes that had been differentiated for 3 or 4 days and treated with either myostatin (10 ng/ml) or activin A (10 ng/ml) in the presence of increasing concentration of BYM338. Shown are means \pm SEMs from 3 or 4 independent experiments.

myoblasts to differentiation medium compared to those for the control culture. This suggests that ligands involved in negative regulation of differentiation are produced by myoblasts during differentiation and act in a paracrine/autocrine manner on muscle cells. Likewise, BYM338 also prevented the inhibition of differentiation and fusion induced upon exogenous addition of myostatin or activin A (Fig. 2A and B). BYM338 also convincingly reversed the increase in Smad2/3 phosphorylation triggered by myostatin stimulation, and it also prevented the subsequent myostatin-induced reduction in P-AKT reported in a previous publication (16) (Fig. 2C). Moreover, myostatin and activin A inhibited myoblast differentiation, as reflected by inhibition of myogenin protein expression after 2 days of differentiation and by a reduction in creatine kinase (CK) activity, with EC_{50} s of 1.67 and 2.71 ng/ml, respectively (Fig. 2D and E). Treating the cells during differentiation with BYM338 increased myogenin levels and blocked the negative effect of myostatin and activin A on the protein levels (Fig. 2D). In addition, BYM338 enhanced differentiation, as measured by determination of an elevation in CK activity. Typically, CK activity has been reported to increase throughout differentia-

tion (32). Administration of BYM338 relieved both the myostatin- and activin A-induced inhibition of differentiation, with IC_{50} s of 519 ± 231 pM and $3,105 \pm 1,114$ pM ($n = 4$ or 5), respectively.

Human primary myotubes were cultured for 7 days in differentiation medium. Myostatin and activin A treatment of these human myotube cultures resulted in significant atrophy in comparison with that for the untreated controls and reduced the myotube diameter and the differentiation index, all of which were at least partially prevented by BYM338 treatment (Fig. 3A and B). When human primary myotubes were treated with myostatin or activin A, phosphorylation and activation of Smad2/3 occurred. Administration of BYM338 significantly reduced the level of Smad2/3 phosphorylation induced by either myostatin or activin A (Fig. 3C). As reported previously (16), subsequent to Smad2/3 phosphorylation, myostatin and activin A caused a negative regulation of the IGF-1/AKT pathway through a reduction of AKT phosphorylation. This again could be restored upon BYM338 administration (Fig. 3D). Lastly, in primary human myotubes, myostatin and activin A induced a significant decrease in myosin heavy chain levels; this may in part be due to a decrease in protein syn-

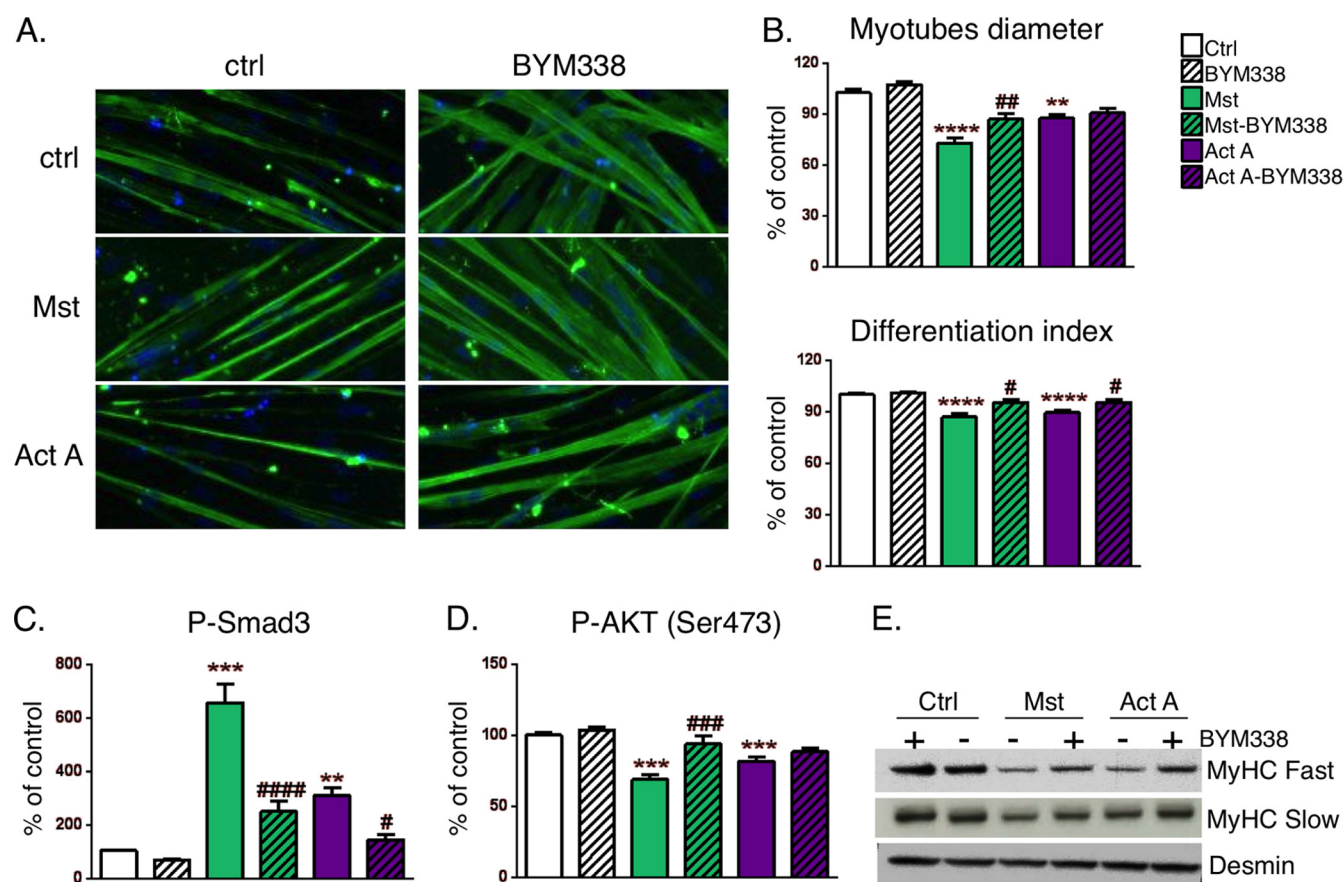


FIG 3 ActRII inhibition relieves myostatin- and activin A-induced atrophy. (A) Human primary myotubes treated for 72 h in the absence (control) and presence of myostatin (100 ng/ml) or activin A (100 ng/ml) alone and in combination with BYM338 (30 μ g/ml) were stained with anti-MyHC antibody and DAPI. Shown are representative pictures. (B) Analysis of myotube diameters was performed as described in Materials and Methods. Data are expressed as a percentage of the value for the control, as indicated in Material and Methods. Shown are means \pm SEMs from 4 independent experiments. Asterisks indicate *P* values versus controls; pound signs indicate *P* values versus samples without BYM338 treatment. **** or ####, *P* < 0.0001; *** or ###, *P* < 0.001; ** or ##, *P* < 0.01; #, *P* < 0.05. (C) The level of Smad3 phosphorylation in myotubes treated for 2 h in the absence (control) and presence of myostatin (100 ng/ml) or activin A (100 ng/ml) alone and in combination with BYM338 (30 μ g/ml) was quantitated using the AlphaScreen SureFire protocol. Shown are means \pm SEMs from 4 independent experiments. Asterisks indicate *P* values versus the control; pound signs indicate *P* values versus samples without BYM338 treatment. (D) Analysis of AKT phosphorylation was performed using a MesoScale Discovery reader in myotubes treated for 24 h. Shown are means \pm SEMs from 6 or 7 independent experiments. (E) Immunoblotting of MyHC from samples of myotubes incubated for 72 h. A blot representative of blots from three independent experiments is shown.

thesis by blocking the AKT/mTOR pathway. This detrimental effect on myotube integrity and content could be prevented by treatment with BYM338 (Fig. 3E).

Skeletal muscle hypertrophy in naive mice. BYM338 administration at 6 and 20 mg/kg for 4 weeks to young SCID mice promoted an increase in body weight and skeletal muscle hypertrophy of all examined muscles, slow, fast, and mixed, in a dose-dependent manner (Fig. 4A and B). Hypertrophy was significant at both 6 and 20 mg/kg, with maximal increases reaching 25% to 50%, depending on the examined muscle. The fiber cross-sectional area distribution of the gastrocnemius/plantaris muscle was significantly increased, reflecting hypertrophy, i.e., an increase in the diameter of individual fibers (Fig. 4C) without changes in fiber numbers (Fig. 4E). Additionally, BYM338 treatment did not significantly alter the fiber type composition of the muscles (Fig. 4D), confirming its ability to induce hypertrophy in all muscle types.

Microarray profiling was used to study the gene expression effect in mouse gastrocnemius muscle after a 4-week treatment

with BYM338 dosed at 20 mg/kg. Despite the strong hypertrophy phenotype observed in the treated animals, only 58 genes were found to be differentially regulated above the level of significance between the treatment and control groups (47 upregulated and 11 downregulated) (Table 1). Interestingly, among the upregulated genes, we found IGF1, a well-known marker of muscle growth. Pathway analysis suggests that BYM338 treatment is associated with extracellular matrix remodeling and downregulation of translation and oxidative phosphorylation (data not shown).

Hypertrophy through inhibition of ligands beyond myostatin. In order to investigate the importance of myostatin inhibition and to determine whether inhibition of other ligands that signal via ActRII was playing a significant role in the hypertrophy induced by BYM338, we first compared the antibody with an inhibitor that neutralizes only myostatin, a stabilized myostatin propeptide (D76A). This type of construct was reported in a prior study (16) and validated to be a myostatin-specific inhibitor. The *in vitro* activity of the myostatin propeptide (D76A) was con-

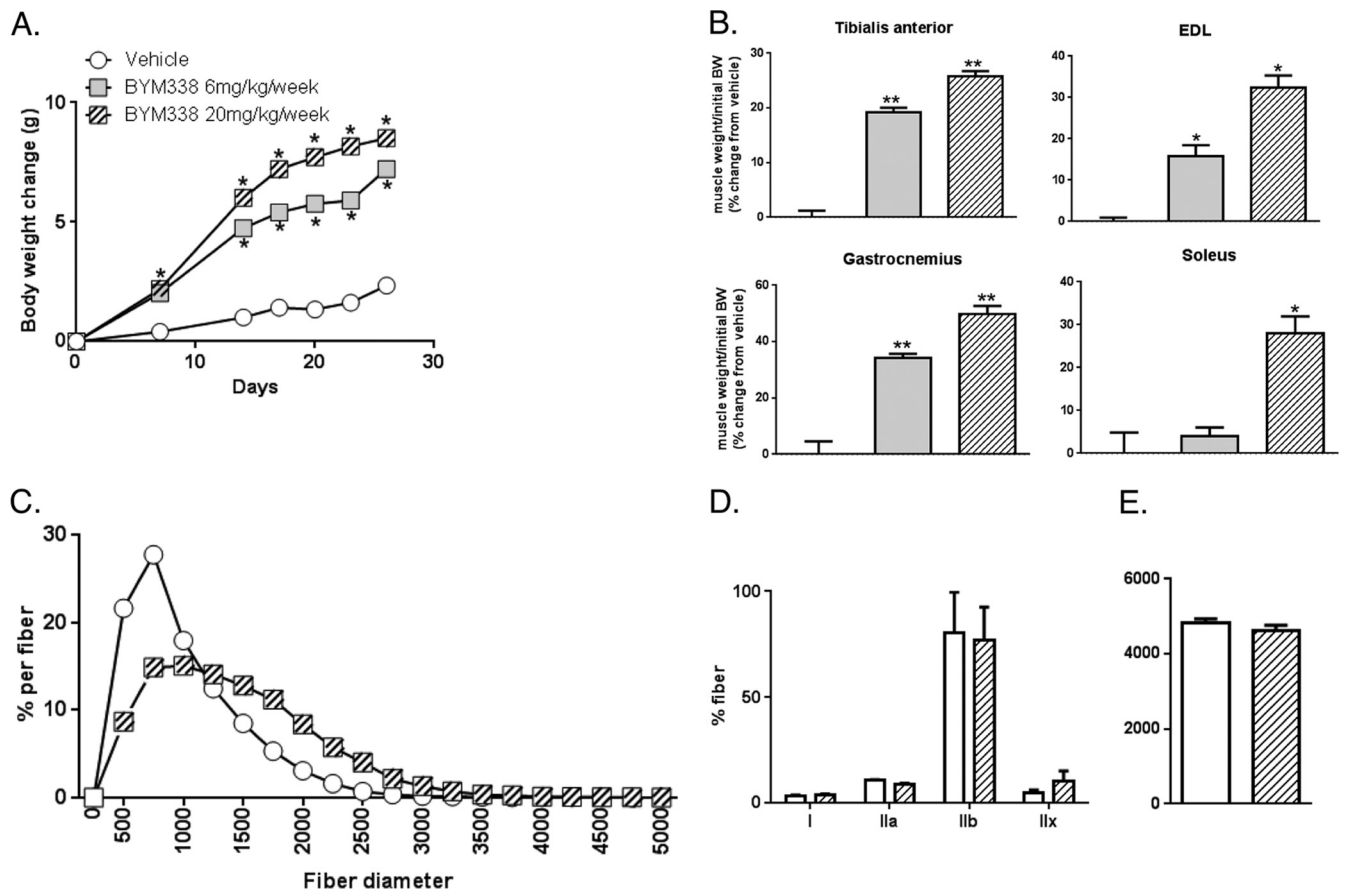


FIG 4 Dose-dependent efficacy of BYM338 in naive SCID mice. (A) Body weight over 4 weeks of treatment with vehicle or BYM338 dosed weekly at 6 or 20 mg/kg. Absolute body weight change values are expressed as means \pm SEMs ($n = 9$ or 10). (B) The weights of the tibialis anterior, EDL, gastrocnemius, and soleus muscles were normalized by the initial body weight (BW). Values are expressed as the mean percent change from the value for the control \pm SEM ($n = 9$ or 10). *, $P < 0.05$ versus the control; **, $P < 0.01$ versus the control (Student's t test). (C) Fiber cross-sectional area of the gastrocnemius muscle with the plantaris muscle. The frequency distributions of the fiber cross-sectional area are plotted. Values are expressed as means \pm SEMs ($n = 4$ or 5). (D) Fiber type distribution in the gastrocnemius muscle from control mice and mice treated with BYM338 at 20 mg/kg. Values are expressed as the percentage of the fiber type \pm SEM ($n = 5$ or 6). (E) Fiber number (indicated on the y axis) in the gastrocnemius muscle from vehicle-treated (white bar) and BYM338 (20 mg/kg)-treated (striped bar) mice expressed as means \pm SEMs ($n = 5$ or 6).

firmed using the CAGA-luciferase reporter gene assay in HEK293 cells described in the legends to Fig. 1B and C and also used to characterize BYM338 (Fig. 5A). Both BYM338 and the myostatin propeptide were administered weekly for 5 weeks to young SCID mice; BYM338 was administered at 10 mg/kg, and the myostatin propeptide was administered at 30 mg/kg (the dose applied was higher than that applied in previously published studies [33, 34]). Body weight increased throughout the treatment period, reaching significance upon BYM338 treatment only (36% versus 15% for myostatin propeptide). The 15% increase induced by the myostatin propeptide is in line with that described in a prior publication (16); the ActRII antibody was over 2-fold more efficacious (Fig. 5B). Muscle weights increased significantly in most muscles examined, with more pronounced increases demonstrated with BYM338 (Fig. 5C). This greater increase in total muscle mass was further corroborated by analyzing the fiber cross-sectional area distribution, demonstrating that the factors were acting by increasing fiber diameter, as opposed to fiber number (Fig. 5D). To further examine the contribution of myostatin blockade to the anabolic effects of BYM338, we administered CDD866, the mouse chimeric equivalent to BYM338, to wt and myostatin mutant

(Mstn^{Ln/Ln}) mice, i.e., mice with a myostatin loss-of-function mutation (35). We detected significant body weight, lean body mass, and muscle weight (Fig. 5E to G) increases in both wild-type and mutant mice upon CDD866 treatment, confirming that BYM338 can induce muscle growth in adult mice by blocking a ligand(s) other than just myostatin.

Prevention of glucocorticoid-induced muscle wasting. Catabolic conditions are often associated with hypercortisolism, which in turn plays a major role in skeletal muscle atrophy (36, 37). Administration of high doses of glucocorticoids induces muscle atrophy and is often associated with elevated myostatin levels (38). The myostatin promoter bears several glucocorticoid response elements, and myostatin deletion has been reported to prevent glucocorticoid-induced muscle wasting (39). The ability of BYM338 to protect muscles from glucocorticoid-induced atrophy and weakness was assessed in a mouse model. BYM338 administered concurrently with the glucocorticoid dexamethasone (DEX) for 2 weeks prevented the loss of muscle mass, tetanic force, and fiber cross-sectional area induced by DEX (Fig. 6A to C, respectively). In addition, BYM338 reduced the level of the E3 ubiquitin ligases induced by DEX, MAFbx, and MuRF1, which contribute to

TABLE 1 Genes differentially expressed upon BYM338 treatment

Probe set identifier	Gene symbol	Gene name	Fold change ^a	Adjusted <i>P</i> value
1423261_at	1500015O10Rik	RIKEN cDNA 1500015O10 gene	2.31	2.39E-03
1435605_at	Actr3b	ARP3 actin-related protein 3 homolog B (<i>Saccharomyces cerevisiae</i>)	2.3	2.38E-10
1416835_s_at	Amd1	S-Adenosylmethionine decarboxylase 1	1.91	1.45E-06
1452106_at	Npnt	Nephronectin	1.86	1.39E-05
1420569_at	Chad	Chondroadherin	1.82	5.51E-03
1449824_at	Prg4	Proteoglycan 4 (megakaryocyte-stimulating factor, articular superficial zone protein)	1.7	2.38E-04
1424268_at	Smox	Spermine oxidase	1.66	2.33E-04
1460555_at	Fam65b	Family with sequence similarity 65, member B	1.54	5.13E-07
1427884_at	Col3a1	Collagen, type III, alpha 1	1.48	6.43E-08
1421186_at	Ccr2	Chemokine (C-C motif) receptor 2	1.48	1.48E-03
1423669_at	Col1a1	Collagen, type I, alpha 1	1.46	5.75E-10
1423110_at	Col1a2	Collagen, type I, alpha 2	1.46	1.90E-08
1448424_at	Frzb	Frizzled-related protein	1.45	8.60E-03
1438009_at	Hist1h2ae	Histone cluster 1, H2ae	1.43	1.08E-04
1423329_at	Gdap1	Ganglioside-induced differentiation-associated protein 1	1.35	3.06E-04
1422789_at	Aldh1a2	Aldehyde dehydrogenase family 1, subfamily A2	1.31	5.12E-04
1433893_s_at	Spag5	Sperm-associated antigen 5	1.29	2.42E-04
1422847_a_at	Prkcd	Protein kinase C, delta	1.29	4.22E-10
1418713_at	Pcbp1	Pterin 4 alpha carbinolamine dehydratase/dimerization cofactor of hepatocyte nuclear factor 1 alpha 1 (TCF1)	1.25	1.90E-08
1416342_at	Tnc	Tenascin C	1.25	7.89E-03
1427239_at	Ift122	Intraflagellar transport 122 homolog (<i>Chlamydomonas</i>)	1.24	1.00E-05
1425039_at	Itgb1	Integrin, beta-like 1	1.24	6.11E-04
1416318_at	Serpinb1a	Serine (or cysteine) peptidase inhibitor, clade B, member 1a	1.22	3.38E-03
1439827_at	Adamts12	A disintegrin-like and metallopeptidase (reprolysin type) with thrombospondin type 1 motif, 12	1.22	7.55E-07
1451410_a_at	Crip3	Cysteine-rich protein 3	1.19	1.18E-04
1416601_a_at	Rcan1	Regulator of calcineurin 1	1.15	4.83E-06
1448328_at	Sh3bp2	SH3 domain binding protein 2	1.14	1.90E-08
1459913_at	Tnfsf10	Tumor necrosis factor (ligand) superfamily, member 10	1.14	7.85E-04
1434479_at	Col5a1	Collagen, type V, alpha 1	1.13	3.55E-10
1419703_at	Col5a3	Collagen, type V, alpha 3	1.12	7.53E-05
1434411_at	Col12a1	Collagen, type XII, alpha 1	1.11	8.54E-03
1451105_at	Vash2	Vasohibin 2	1.1	1.33E-04
1442019_at	Rcvrn	Recoverin	1.1	1.45E-03
1428420_a_at	1200009I06Rik	RIKEN cDNA 1200009I06 gene	1.07	5.20E-04
1434997_at	Cdk19	Cyclin-dependent kinase 19	1.05	2.13E-10
1451353_at	Tm6sf1	Transmembrane 6 superfamily member 1	1.05	1.47E-05
1460248_at	Cpxm2	Carboxypeptidase X2 (M14 family)	1.04	2.82E-03
1429566_a_at	Hipk2	Homeodomain-interacting protein kinase 2	1.03	2.11E-08
1421926_at	Mapk11	Mitogen-activated protein kinase 11	1.03	7.47E-05
1425156_at	Gbp7	Guanylate binding protein 7	1.02	5.30E-03
1429553_at	Cilp2	Cartilage intermediate layer protein 2	1.01	8.92E-03
1448698_at	Ccnd1	Cyclin D1	1.01	3.81E-03
1421851_at	Mtap1b	Microtubule-associated protein 1B	1	1.13E-02
1425631_at	Ppp1r3c	Protein phosphatase 1, regulatory (inhibitor) subunit 3C	1	8.77E-03
1424870_at	Osbpl10	Oxysterol binding protein-like 10	0.98	7.72E-07
1419519_at	Igf1	Insulin-like growth factor 1	0.98	1.96E-07
1460218_at	Cd52	CD52 antigen	0.98	9.29E-03
1444128_at	Arhgap26	Rho GTPase-activating protein 26	-1.09	1.06E-04
1434628_a_at	C230052I12Rik	RIKEN cDNA C230052I12 gene	-1.12	5.02E-09
1417155_at	Mycn	v-myc myelocytomatosis virus-related oncogene, neuroblastoma derived (avian)	-1.25	1.66E-03
1454995_at	Ddah1	Dimethylarginine dimethylaminohydrolase 1	-1.37	7.72E-07
1422580_at	Myl4	Myosin, light polypeptide 4	-1.4	1.72E-06
1416383_a_at	Pcx	Pyruvate carboxylase	-1.41	2.62E-06
1428352_at	Arrdc2	Arrestin domain containing 2	-1.44	2.43E-03
1445186_at	Stc2	Stanniocalcin 2	-1.49	2.67E-05
1418697_at	Inmt	Indolethylamine N-methyltransferase	-1.64	1.95E-04
1447016_at	Tbc1d1	TBC1 domain family, member 1	-2.36	1.88E-06
1432001_at	Zmynd17	Zinc finger, MYND domain containing 17	-2.61	3.92E-04

^a Fold changes are expressed in log₂ scale.

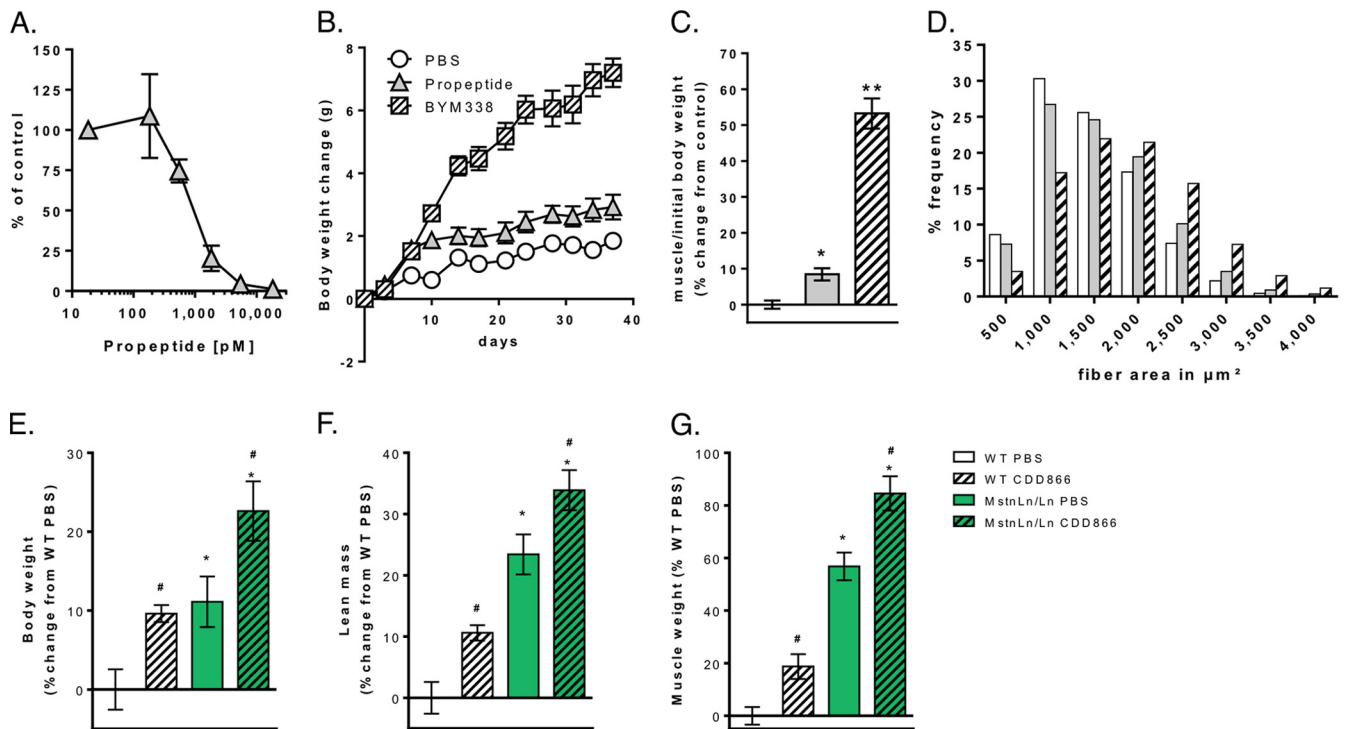


FIG 5 Comparison of efficacy of anti-ActRII antibody treatment versus pharmacological or genetic myostatin inhibition. (A) Inhibition of CAGA-luciferase reporter gene activity induced with 10 ng/ml myostatin with various concentrations of mutant D76A propeptide. (B) Body weight. (C and D) Weight of the gastrocnemius muscle with the plantaris muscle (C) and cross-sectional area of the gastrocnemius muscle (D) from naive SCID mice administered BYM338 (10 mg/kg; striped bar), myostatin propeptide D76A (30 mg/kg; gray bar), or PBS (white bar) i.p. weekly for 5 weeks with an additional administration on day 3. Muscle weight was normalized to the initial body weight measured on day 0. Absolute body weight change values are expressed as means \pm SEMs ($n = 9$ or 10). *, $P < 0.05$ versus the group treated with PBS; **, $P < 0.01$ versus the group treated with PBS (Dunnett's test following ANOVA). (E to G) Body weight (E), lean mass (F), and tibialis anterior muscle weight (G) of wild-type mice ($n = 10$ /group) and Mstn^{Ln/Ln} mice ($n = 8$ /group) administered CDD866, murinized BYM338 (20 mg/kg), or PBS s.c. weekly on days 0, 7, 14, 21, and 28. Body weight and lean mass were measured on day 0 and day 21 using a mouse body composition NMR analyzer. Data are presented as the mean \pm SEM and were analyzed with a one-way ANOVA with a Bonferroni *post hoc* test. *, $P < 0.05$ compared with wt with the same treatment; #, $P < 0.05$ compared with vehicle-treated mice with the same genotype. Muscle weights are expressed as the percent difference from the results for wt mice treated with vehicle.

muscle atrophy by degrading key substrates (40–42) (Fig. 6D). Furthermore, when administered after 3 weeks of DEX treatment and DEX withdrawal, two weekly doses of BYM338 were able to dose dependently enhance the recovery of skeletal muscle mass (Fig. 6E).

These findings demonstrate that use of BYM338 can facilitate recovery from or prevent skeletal muscle atrophy and weakness under conditions associated with hypercortisolism.

DISCUSSION

There is a dearth of available treatments for disease-, age-, and injury-related loss of skeletal muscle. Skeletal muscle atrophy results in weakness and frailty. Also, it appears in the form of cachexia associated with serious conditions, such as cancer, chronic obstructive pulmonary disease (COPD), and chronic kidney disease (CKD). The presence of cachexia is a significant risk factor predicting an increased likelihood of death from these already serious conditions. Indeed, it was demonstrated in a mouse model of cancer cachexia that a muscle-sparing treatment, use of the ActRIIB trap, which prevented the loss of skeletal muscle but did not affect tumor mass, nevertheless resulted in a significant improvement in survival (24). Furthermore, the loss of skeletal muscle mass associated with old age, called “sarcopenia,” is well documented, and the resulting frailty is a major cause of morbidity

and mortality in the rapidly increasing aged population (2). Thus, it should not be surprising that effective treatments resulting in sparing of skeletal muscle under disease conditions are actively being sought.

The simple blockade of myostatin was among the earliest and most obvious treatment strategies. This is because of the dramatic hypertrophy seen in a variety of myostatin-null animals and in a human who was null for this ligand (5–9). Some interesting correlations between myostatin levels and cachexic muscle loss have been reported in preclinical mouse models, as well as in human diseases (43). However, the levels of myostatin reported in humans are lower than those seen in rodents (44–46), and even in rodents, more modest effects are seen when myostatin is blocked in adult animals (33, 47) than when it is blocked during development. These findings raise the question as to the effectiveness that one might expect from blocking myostatin alone, as opposed to, in addition, inhibiting the other ligands that contribute to the negative regulation of muscle mass by signaling through the same receptor. Indeed, specific treatment with an antimyostatin antibody, JA16 (10), resulted in just a 15% increase in muscle mass, much less than that observed in the knockout animals; this perhaps suggests that myostatin's major role is during development and opens up the possibility that other factors are either more

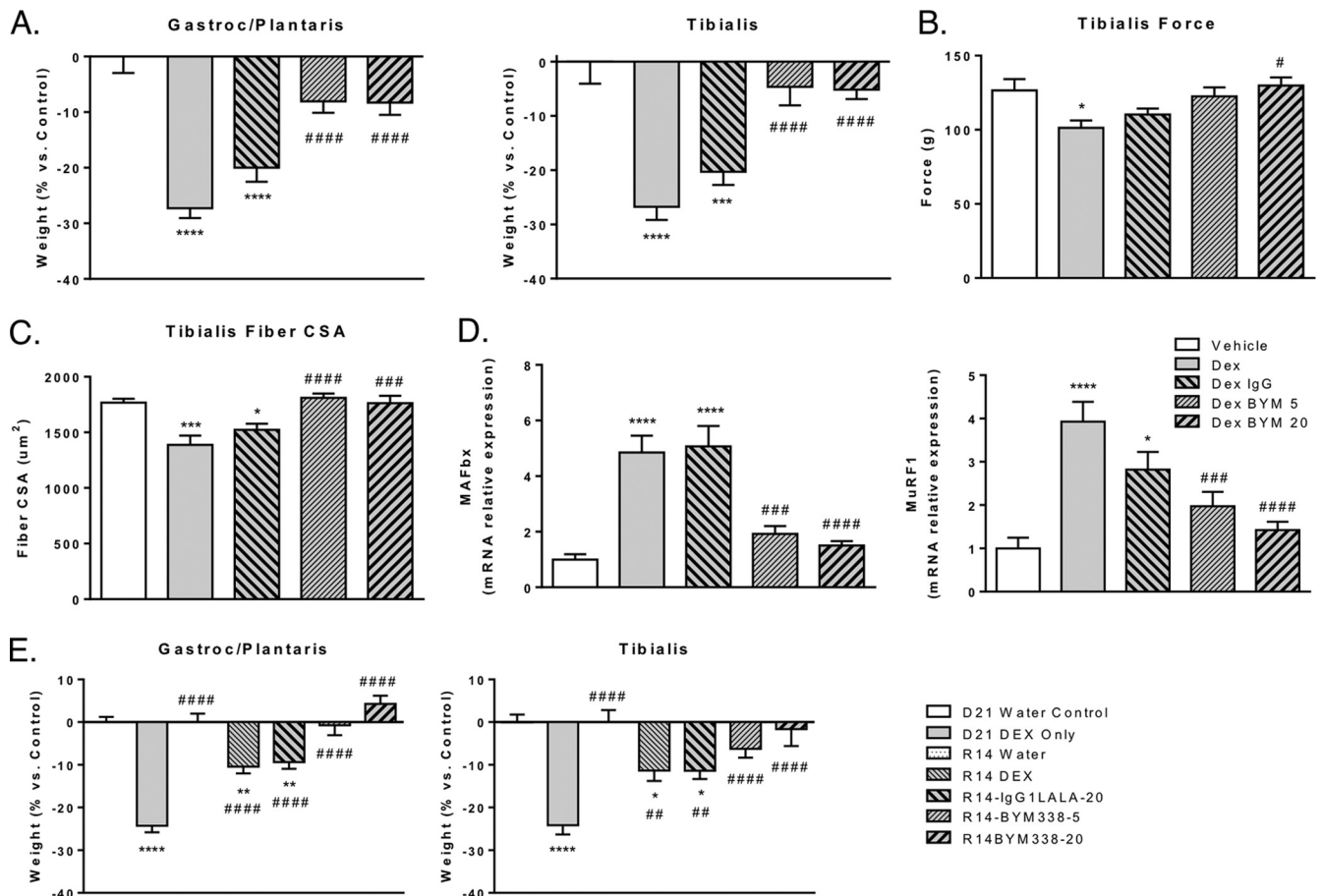


FIG 6 Anti-ActRII antibody efficacy at preventing (A to D) and reversing (E) glucocorticoid-induced atrophy. (A) Weights of the gastrocnemius/plantaris (Gastroc/Plantaris) and tibialis craniialis muscles expressed as the percent difference relative to the weights for the water-treated control group; (B) evoked peak tetanic force of the tibialis craniialis muscle; (C) mean cross-sectional area (CSA) of muscle fibers in the tibialis craniialis muscle; (D) MAFbx and MuRF1 mRNA expression in the tibialis craniialis muscle relative to that in the control group after 14 days of treatment with DEX at ~2.4 mg/kg/day in drinking water coadministered with BYM338 at 5 and 20 mg/kg or the IgG1-LALA isotype at 20 mg/kg i.p. at days 0, 2, and 7. (E) Weights of the gastrocnemius/plantaris and tibialis craniialis muscles, expressed as the percent difference relative to the water-treated control group, from mice that received DEX daily in the drinking water at ~2.4 mg/kg/day for 21 days and administered BYM338 at 5 and 20 mg/kg or the IgG1-LALA isotype at 20 mg/kg i.p. on days 21, 23, and 28. Data are presented as means \pm SEMs ($n = 7$ to 10). Group means were compared by one-way ANOVA followed by Tukey's or Dunnett's multiple-comparison test, as appropriate. Differences were considered significant at P values of ≤ 0.05 (*, **, ***, and ****, $P < 0.05$, 0.01, 0.001, and 0.0001 versus the group treated with vehicle, respectively; #, ##, ###, and ####, $P < 0.05$, 0.01, 0.001, and 0.0001 versus the group treated with DEX, respectively).

important or at least also contribute to the adult maintenance of skeletal muscle mass. This implication was strengthened by the genetic cross of the myostatin-null mouse with a follistatin transgenic animal, resulting in much greater hypertrophy (48). These data clearly indicated that factors beyond myostatin which could still bind follistatin, such as the activins, play a role in the control of muscle size. Finally, in a direct experiment, it was shown that in addition to myostatin, the closely related GDF11 and the activins all were capable of inhibiting myoblast differentiation and causing myotube atrophy (16), further implicating the ActRII receptors as potential targets for therapeutic blockade.

Therefore, we produced a human antibody to the ActRII receptors, BYM338, which binds ActRIIB at least 200-fold better than it binds ActRIIA (given the relative dissociation equilibrium constants of 1.7 pM versus 434 pM, respectively). This antibody was capable of inhibiting the activity of myostatin and the activins on skeletal myoblasts and myotubes, as demonstrated by a decrease in the Smad2/3 phosphorylation and subsequent gene ex-

pression activation caused by the Smad transcription factors. BYM338 also restored the AKT-mediated signaling inhibited by these ligands. This restoration of AKT phosphorylation is important, since AKT has been shown in prior studies to be required for weight-bearing-induced skeletal muscle hypertrophy; we have also previously shown that AKT activates mTOR-mediated phosphorylation of p70S6 kinase in skeletal muscle (49) and inhibits GSK3, resulting in muscle hypertrophy (50). However, administration of an ActRIIB receptor trap to AKT1- and AKT2-deficient mice still induced a significant increase in muscle mass, demonstrating that there are additional, AKT-independent pathways which contribute to the overall hypertrophic phenotype (21).

BYM338 resulted in significant skeletal muscle hypertrophy when administered *in vivo*. The sparing of skeletal muscle was accompanied by an increase in the muscle fiber diameter, demonstrating that the effect is via true hypertrophy, as opposed to hyperplasia. Hypertrophy was clearly demonstrated in all examined muscles and in all fiber types, fast or slow.

In comparison to a myostatin-propeptide construct, which blocks myostatin only, the antibody produced a dramatically better response: more than 2-fold the hypertrophy seen with myostatin blockade alone. Furthermore, BYM338 could induce hypertrophy in a myostatin-null animal, further demonstrating that in adult animals myostatin is not the only TGF- β family member controlling muscle mass. Prior studies had suggested this as well (10, 18), but this is the first demonstration that an antibody directed at the ActRII receptor can induce significantly greater hypertrophy than myostatin inhibition alone; the point had been made with the ActRIIB trap, but that molecule can actually also bind other ligands that can signal through distinct TGF- β family member receptors (13). A microarray analysis for genes perturbed to a significant degree in gastrocnemius muscle after 4 weeks of treatment demonstrated an upregulation of IGF-1, providing an interesting point of cross talk between the pathways. This finding provides a further mechanism as to how ActRII inhibition results in restoration of AKT signaling.

The ability to induce skeletal muscle hypertrophy in a healthy animal does not necessarily translate into efficacy in a disease condition, since there is no guarantee that a prohypertrophy mechanism will be dominant over the pathways inducing skeletal muscle atrophy. Therefore, the glucocorticoid dexamethasone (DEX) was used to induce muscle atrophy. Many cachectic settings are accompanied by high cortisol levels, including COPD, kidney cachexia, and acute severe burns (36, 37, 51). Also, simple treatment with high doses of glucocorticoids for therapeutic purposes, such as when there is a traumatic brain injury, is sufficient to induce skeletal muscle atrophy (52). In settings of DEX-induced atrophy, BYM338 was able to both prevent the loss of skeletal muscle mass when given coincident with the glucocorticoid and enhance the recovery from muscle atrophy when administered after the atrophy occurred. BYM338 also significantly preserved muscle function, as DEX-induced atrophy led to a tetanic force loss of more than 20%, which was fully reversed by BYM338 treatment. There is some controversy regarding an increase in specific force in myostatin-deficient mice, since the overall increase in mass is so large that while an increase in total force is achieved, the force per mass is actually lower; this could be due to the awkward angling of the fibers in the grossly hypertrophic tissue combined with the lack of actual training of the muscle in these animals (53); nevertheless, there is clear evidence of improved muscle function in other settings of reduced myostatin, such as in whippet dogs, where heterozygous myostatin mutant animals display an impressive increase in muscle mass coupled to increased performance, i.e., racing speed (9). Altogether, soluble ActRIIB-Fc administered to AKT1- or AKT2-knockout mice positively regulated muscle size, strength, and contraction (21). Similarly, protection from cancer cachexia using pharmacological intervention with soluble ActRIIB-Fc has been demonstrated through preservation of both muscle mass and function (54).

The demonstration of preclinical efficacy with a blocking antibody to ActRII establishes a middle ground between the restricted blockade of myostatin, on the one hand, and the use of an ActRIIB soluble receptor as a trap, on the other hand, which can be a sink for ligands such as BMP9/10, binding additional receptors like BMPRII/Alk1 (13).

The data presented in this study suggest that the BYM338 antibody could be an effective treatment for important clinical set-

tings of skeletal muscle atrophy. Furthermore, on the basis of recent findings, blockade of activin type II receptors via an antibody approach may also represent a novel therapeutic modality to aid in switching the metabolic balance between adiposity and muscularity, since an increase in skeletal muscle mass via inhibition of the myostatin pathway was accompanied by a decrease in white adipose tissue in mice on a normal or high-fat diet (55). One recently identified mechanism helping to explain this effect is that an ActRIIB antibody has been shown to induce a functional increase in brown fat (56), resulting in enhanced heat production by actually increasing the lipid content in the brown fat tissue (56). Therefore, the potential metabolic benefit of an anti-ActRII antibody approach may relate to a combined increase of functional lean body mass and brown fat. Finally, there have been suggestions that ActRIIB inhibition can also be helpful in settings of heart failure (43) and in those settings where inflammatory cytokines induce muscle loss; under such conditions, there is an interesting cross talk between the cytokine pathway and TGF- β signaling, since downstream of NF- κ B in the cytokine pathway, there is an induction of activin A production in the muscle, causing muscle atrophy. Therefore, the ActRII antibody approach should be uniquely effective in preventing atrophy induced by inflammation (16).

In summary, there are quite a few settings where inhibition of the ActRII pathway may be of benefit. Such treatments are clearly needed, given the complete and surprising lack of effective options for patients with muscle loss, frailty, and weakness.

ACKNOWLEDGMENTS

We thank the Muscle Diseases Group, in particular, Ulrike Trendelenburg's laboratory, and the Protein Production Group, at NIBR for their enthusiastic support, along with the rest of the NIBR community, in particular, Mark Fishman and Michaela Kneissel. We also thank Chris Lu for his early contribution on the project and the Protein Production Group for their long-standing support. We thank MorphoSys for its contributions to the isolation and characterization of the BYM338 antibody.

We all were Novartis Pharma AG employees at the time of work completion.

REFERENCES

1. Bodine SC. 2013. Disuse-induced muscle wasting. *Int. J. Biochem. Cell Biol.* 45:2200–2208. <http://dx.doi.org/10.1016/j.biocel.2013.06.011>.
2. Morley JE. 2012. Sarcopenia in the elderly. *Fam. Pract.* 29:i44–i48. <http://dx.doi.org/10.1093/fampra/cmr063>.
3. Glass D, Roubenoff R. 2010. Recent advances in the biology and therapy of muscle wasting. *Ann. N. Y. Acad. Sci.* 1211:25–36. <http://dx.doi.org/10.1111/j.1749-6632.2010.05809.x>.
4. Han HQ, Zhou X, Mitch WE, Goldberg AL. 2013. Myostatin/activin pathway antagonism: molecular basis and therapeutic potential. *Int. J. Biochem. Cell Biol.* 45:2333–2347. <http://dx.doi.org/10.1016/j.biocel.2013.05.019>.
5. McPherron AC, Lawler AM, Lee SJ. 1997. Regulation of skeletal muscle mass in mice by a new TGF-beta superfamily member. *Nature* 387:83–90. <http://dx.doi.org/10.1038/387083a0>.
6. McPherron AC, Lee SJ. 1997. Double muscling in cattle due to mutations in the myostatin gene. *Proc. Natl. Acad. Sci. U. S. A.* 94:12457–12461. <http://dx.doi.org/10.1073/pnas.94.23.12457>.
7. Schuelke M, Wagner KR, Stolz LE, Hubner C, Riebel T, Komen W, Braun T, Tobin JF, Lee SJ. 2004. Myostatin mutation associated with gross muscle hypertrophy in a child. *N. Engl. J. Med.* 350:2682–2688. <http://dx.doi.org/10.1056/NEJMoa040933>.
8. Clop A, Marcq F, Takeda H, Pirottin D, Tordoir X, Bibe B, Bouix J, Caiment F, Elsen JM, Eyche F, Larzul C, Laville E, Meish F, Milenkovic D, Tobin J, Charlier C, Georges M. 2006. A mutation creating a potential illegitimate microRNA target site in the myostatin gene affects muscularity in sheep. *Nat. Genet.* 38:813–818. <http://dx.doi.org/10.1038/ng1810>.

9. Mosher DS, Quignon P, Bustamante CD, Sutter NB, Mellersh CS, Parker HG, Ostrander EA. 2007. A mutation in the myostatin gene increases muscle mass and enhances racing performance in heterozygote dogs. *PLoS Genet.* 3:e79. <http://dx.doi.org/10.1371/journal.pgen.0030079>.
10. Lee SJ, Reed LA, Davies MV, Girgenrath S, Goad ME, Tomkinson KN, Wright JF, Barker C, Ehrmantraut G, Holmstrom J, Trowell B, Gertz B, Jiang MS, Sebald SM, Matzuk M, Li E, Liang LF, Quattlebaum E, Stotish RL, Wolfman NM. 2005. Regulation of muscle growth by multiple ligands signaling through activin type II receptors. *Proc. Natl. Acad. Sci. U. S. A.* 102:18117–18122. <http://dx.doi.org/10.1073/pnas.0505996102>.
11. Lee SJ, Lee YS, Zimmers TA, Soleimani A, Matzuk MM, Tsuchida K, Cohn RD, Barton ER. 2010. Regulation of muscle mass by follistatin and activins. *Mol. Endocrinol.* 24:1998–2008. <http://dx.doi.org/10.1210/me.2010-0127>.
12. Trendelenburg AU, Meyer A, Jacobi C, Feige JN, Glass DJ. 2012. TAK-1/p38/nf-kappaB signaling inhibits myoblast differentiation by increasing levels of activin A. *Skelet. Muscle* 2:3. <http://dx.doi.org/10.1186/2044-5040-2-3>.
13. Souza TA, Chen X, Guo Y, Sava P, Zhang J, Hill JJ, Yaworsky PJ, Qiu Y. 2008. Proteomic identification and functional validation of activins and bone morphogenetic protein 11 as candidate novel muscle mass regulators. *Mol. Endocrinol.* 22:2689–2702. <http://dx.doi.org/10.1210/me.2008-0290>.
14. McPherron AC, Huynh TV, Lee SJ. 2009. Redundancy of myostatin and growth/differentiation factor 11 function. *BMC Dev. Biol.* 9:24. <http://dx.doi.org/10.1186/1471-213X-9-24>.
15. Gamer LW, Cox KA, Small C, Rosen V. 2001. Gdf11 is a negative regulator of chondrogenesis and myogenesis in the developing chick limb. *Dev. Biol.* 229:407–420. <http://dx.doi.org/10.1006/dbio.2000.9981>.
16. Trendelenburg AU, Meyer A, Rohner D, Boyle J, Hatakeyama S, Glass DJ. 2009. Myostatin reduces Akt/TORC1/p70S6K signaling, inhibiting myoblast differentiation and myotube size. *Am. J. Physiol. Cell Physiol.* 296:C1258–C1270. <http://dx.doi.org/10.1152/ajpcell.00105.2009>.
17. Rebbapragada A, Benchabane H, Wrana JL, Celeste AJ, Attisano L. 2003. Myostatin signals through a transforming growth factor [beta]-like signaling pathway to block adipogenesis. *Mol. Cell. Biol.* 23:7230–7242. <http://dx.doi.org/10.1128/MCB.23.20.7230-7242.2003>.
18. Lee SJ, McPherron AC. 2001. Regulation of myostatin activity and muscle growth. *Proc. Natl. Acad. Sci. U. S. A.* 98:9306–9311. <http://dx.doi.org/10.1073/pnas.151270098>.
19. Sartori R, Milan G, Patron M, Mammucari C, Blaauw B, Abraham R, Sandri M. 2009. Smad2 and 3 transcription factors control muscle mass in adulthood. *Am. J. Physiol. Cell Physiol.* 296:C1248–C1257. <http://dx.doi.org/10.1152/ajpcell.00104.2009>.
20. Glass D. 2010. PI3 kinase regulation of skeletal muscle hypertrophy and atrophy. *Curr. Top. Microbiol. Immunol.* 346:267–278. http://dx.doi.org/10.1007/82_2010_78.
21. Goncalves MD, Pistilli EE, Balduzzi A, Birnbaum MJ, Lachey J, Khurana TS, Ahima RS. 2010. Akt deficiency attenuates muscle size and function but not the response to ActRIIB inhibition. *PLoS One* 5:e12707. <http://dx.doi.org/10.1371/journal.pone.0012707>.
22. Terpos E, Kastritis E, Christoulas D, Gkotszamanidou M, Eleutherakis-Papaikovou E, Kanellias N, Papatheodorou A, Dimopoulos MA. 2012. Circulating activin-A is elevated in patients with advanced multiple myeloma and correlates with extensive bone involvement and inferior survival; no alterations post-lenalidomide and dexamethasone therapy. *Ann. Oncol.* 23:2681–2686. <http://dx.doi.org/10.1093/annonc/mds068>.
23. Hoda MA, Munzker J, Ghanim B, Schelch K, Klinkovits T, Laszlo V, Sahin E, Bedeir A, Lackner A, Dome B, Setinek U, Filipits M, Eisenbauer M, Kenessey I, Torok S, Garay T, Hegedus B, Catania A, Taghavi S, Klepetko W, Berger W, Grusch M. 2012. Suppression of activin A signals inhibits growth of malignant pleural mesothelioma cells. *Br. J. Cancer* 107:1978–1986. <http://dx.doi.org/10.1038/bjc.2012.519>.
24. Zhou X, Wang JL, Lu J, Song Y, Kwak KS, Jiao Q, Rosenfeld R, Chen Q, Boone T, Simonet WS, Lacey DL, Goldberg AL, Han HQ. 2010. Reversal of cancer cachexia and muscle wasting by ActRIIB antagonism leads to prolonged survival. *Cell* 142:531–543. <http://dx.doi.org/10.1016/j.cell.2010.07.011>.
25. Whittemore LA, Song K, Li X, Aghajanian J, Davies M, Girgenrath S, Hill JJ, Jalenak M, Kelley P, Knight A, Maylor R, O'Hara D, Pearson A, Quazi A, Ryerson S, Tan XY, Tomkinson KN, Veldman GM, Widom A, Wright JF, Wudyka S, Zhao L, Wolfman NM. 2003. Inhibition of myostatin in adult mice increases skeletal muscle mass and strength. *Biochem. Biophys. Res. Commun.* 300:965–971. [http://dx.doi.org/10.1016/S0006-291X\(02\)02953-4](http://dx.doi.org/10.1016/S0006-291X(02)02953-4).
26. Bogdanovich S, Perkins KJ, Krag TOB, Whittemore LA, Khurana TS. 2005. Myostatin propeptide-mediated amelioration of dystrophic pathophysiology. *FASEB J.* 19:543–549. <http://dx.doi.org/10.1096/fj.04-2796com>.
27. Attie KM, Borgstein NG, Yang Y, Condon CH, Wilson DM, Pearsall AE, Kumar R, Willins DA, Seehra JS, Sherman ML. 2013. A single ascending-dose study of muscle regulator ace-031 in healthy volunteers. *Muscle Nerve* 47:416–423. <http://dx.doi.org/10.1002/mus.23539>.
28. Haenel C, Satzger M, Ducata DD, Ostendorp R, Brocks B. 2005. Characterization of high-affinity antibodies by electrochemiluminescence-based equilibrium titration. *Anal. Biochem.* 339:182–184. <http://dx.doi.org/10.1016/j.ab.2004.12.032>.
29. National Research Council. 1995. Guide for the care and use of laboratory animals, 7th ed. National Academies Press, Washington, DC.
30. Ibeunjo C, Chick JM, Kendall T, Eash JK, Li C, Zhang Y, Vickers C, Wu Z, Clarke BA, Shi J, Cruz J, Fournier B, Brachet S, Gutzwiller S, Ma Q, Markovits J, Broome M, Steinkrauss M, Skuba E, Galarneau JR, Gygi SP, Glass DJ. 2013. Genomic and proteomic profiling reveals reduced mitochondrial function and disruption of the neuromuscular junction driving rat sarcopenia. *Mol. Cell. Biol.* 33:194–212. <http://dx.doi.org/10.1128/MCB.01036-12>.
31. Lukjanenko L, Brachet S, Pierrel E, Lach-Trifilieff E, Feige JN. 2013. Genomic profiling reveals that transient adipogenic activation is a hallmark of mouse models of skeletal muscle regeneration. *PLoS One* 8:e71084. <http://dx.doi.org/10.1371/journal.pone.0071084>.
32. Grohmann M, Foulstone E, Welsh G, Holly J, Shield J, Crowne E, Stewart C. 2005. Isolation and validation of human prepubertal skeletal muscle cells: maturation and metabolic effects of IGF-I, IGFBP-3 and TNF α . *J. Physiol.* 568:229–242. <http://dx.doi.org/10.1113/jphysiol.2005.093906>.
33. Wolfman NM, McPherron AC, Pappano WN, Davies MV, Song K, Tomkinson KN, Wright JF, Zhao L, Sebald SM, Greenspan DS, Lee SJ. 2003. Activation of latent myostatin by the BMP-1/tolloid family of metalloproteinases. *Proc. Natl. Acad. Sci. U. S. A.* 100:15842–15846. <http://dx.doi.org/10.1073/pnas.2534946100>.
34. Li Z, Zhao B, Kim YS, Hu CY, Yang J. 2010. Administration of a mutated myostatin propeptide to neonatal mice significantly enhances skeletal muscle growth. *Mol. Reprod. Dev.* 77:76–82. <http://dx.doi.org/10.1002/mrd.21111>.
35. Wilkes JJ, Lloyd DJ, Gekakis N. 2009. Loss-of-function mutation in myostatin reduces tumor necrosis factor alpha production and protects liver against obesity-induced insulin resistance. *Diabetes* 58:1133–1143. <http://dx.doi.org/10.2337/db08-0245>.
36. Anker SD, Clark AL, Kemp M, Salsbury C, Teixeira MM, Hellewell PG, Coats AJS. 1997. Tumor necrosis factor and steroid metabolism in chronic heart failure: possible relation to muscle wasting. *J. Am. Coll. Cardiol.* 30:997–1001. [http://dx.doi.org/10.1016/S0735-1097\(97\)00262-3](http://dx.doi.org/10.1016/S0735-1097(97)00262-3).
37. Fitts RH, Romatowski JG, Peters JR, Paddon-Jones D, Wolfe RR, Ferrando AA. 2007. The deleterious effects of bed rest on human skeletal muscle fibers are exacerbated by hypercortisolemia and ameliorated by dietary supplementation. *Am. J. Physiol. Cell Physiol.* 293:C313–C320. <http://dx.doi.org/10.1152/ajpcell.00573.2006>.
38. Ma K, Mallidis C, Bhasin S, Mahabadi V, Artaza J, Gonzalez-Cadavid N, Arias J, Salehian B. 2003. Glucocorticoid-induced skeletal muscle atrophy is associated with upregulation of myostatin gene expression. *Am. J. Physiol. Endocrinol. Metab.* 285:E363–E371. <http://dx.doi.org/10.1152/ajpendo.00487.2002>.
39. Gilson H, Schakman O, Combaret L, Lause P, Grobet L, Attaix D, Ketelslegers JM, Thissen JP. 2007. Myostatin gene deletion prevents glucocorticoid-induced muscle atrophy. *Endocrinology* 148:452–460. <http://dx.doi.org/10.1210/en.2006-0539>.
40. Clarke BA, Drujan D, Willis MS, Murphy LO, Corpina RA, Burova E, Rakhilin SV, Stitt TN, Patterson C, Latres E, Glass DJ. 2007. The E3 ligase MuRF1 degrades myosin heavy chain protein in dexamethasone-treated skeletal muscle. *Cell Metab.* 6:376–385. <http://dx.doi.org/10.1016/j.cmet.2007.09.009>.
41. Cohen S, Brault JJ, Gygi SP, Glass DJ, Valenzuela DM, Gartner C, Latres E, Goldberg AL. 2009. During muscle atrophy, thick, but not thin, filament components are degraded by MuRF1-dependent ubiquitylation. *J. Cell Biol.* 185:1083–1095. <http://dx.doi.org/10.1083/jcb.200901052>.
42. Polge C, Heng AE, Jarzaguet M, Ventadour S, Claustre A, Combaret L, Béchet, D, Matondo M, Uutenweiler-Joseph S, Monsarrat B, Attaix D,

- Taillandier D. 2011. Muscle actin is polyubiquitinated in vitro and in vivo and targeted for breakdown by the E3 ligase MuRF1. *FASEB J.* 25: 3790–3802. <http://dx.doi.org/10.1096/fj.11-180968>.
43. Elliott B, Renshaw D, Getting S, Mackenzie R. 2012. The central role of myostatin in skeletal muscle and whole body homeostasis. *Acta Physiol.* 205:324–340. <http://dx.doi.org/10.1111/j.1748-1716.2012.02423.x>.
 44. Zimmers TA, Davies MV, Koniaris LG, Haynes P, Esquela AF, Tomkinson KN, McPherron AC, Wolfman NM, Lee SJ. 2002. Induction of cachexia in mice by systemically administered myostatin. *Science* 296: 1486–1488. <http://dx.doi.org/10.1126/science.1069525>.
 45. Lakshman KM, Bhasin S, Corcoran C, Collins-Racie LA, Tchistiakova L, Forlow SB, St Ledger K, Burczynski ME, Dorner AJ, Lavallie ER. 2009. Measurement of myostatin concentrations in human serum: circulating concentrations in young and older men and effects of testosterone administration. *Mol. Cell. Endocrinol.* 302:26–32. <http://dx.doi.org/10.1016/j.mce.2008.12.019>.
 46. Wagner KR, Fleckenstein JL, Amato AA, Barohn RJ, Bushby K, Escolar DM, Flanigan KM, Pestronk A, Tawil R, Wolfe GI, Eagle M, Florence JM, King WM, Pandya S, Straub V, Juneau P, Meyers K, Csimma C, Araujo T, Allen R, Parsons SA, Wozney JM, LaVallie ER, Mendell JR. 2008. A phase I/II trial of MYO-029 in adult subjects with muscular dystrophy. *Ann. Neurol.* 63:561–571. <http://dx.doi.org/10.1002/ana.21338>.
 47. Welle S, Bhatt K, Pinkert CA, Tawil R, Thornton CA. 2007. Muscle growth after postdevelopmental myostatin gene knockout. *Am. J. Physiol. Endocrinol. Metab.* 292:E985–E991. <http://dx.doi.org/10.1152/ajpendo.00531.2006>.
 48. Lee SJ. 2007. Quadrupling muscle mass in mice by targeting TGF-beta signaling pathways. *PLoS One* 2:e789. <http://dx.doi.org/10.1371/journal.pone.0000789>.
 49. Bodine SC, Stitt TN, Gonzalez M, Kline WO, Stover GL, Bauerlein R, Zlotchenko E, Scrimgeour A, Lawrence JC, Glass DJ, Yancopoulos GD. 2001. Akt/mTOR pathway is a crucial regulator of skeletal muscle hypertrophy and can prevent muscle atrophy in vivo. *Nat. Cell Biol.* 3:1014–1019. <http://dx.doi.org/10.1038/ncb1101-1014>.
 50. Rommel C, Bodine SC, Clarke BA, Rossman R, Nunez L, Stitt TN, Yancopoulos GD, Glass DJ. 2001. Mediation of IGF-1-induced skeletal myotube hypertrophy by PI(3)K/Akt/mTOR and PI(3)K/Akt/GSK3 pathways. *Nat. Cell Biol.* 3:1009–1013. <http://dx.doi.org/10.1038/ncb1101-1009>.
 51. Pereira C, Murphy K, Jeschke M, Herndon DN. 2005. Post burn muscle wasting and the effects of treatments. *Int. J. Biochem. Cell Biol.* 37:1948–1961. <http://dx.doi.org/10.1016/j.biocel.2005.05.009>.
 52. Deutschman CS, Konstantinides FN, Raup S, Cerra FB. 1987. Physiological and metabolic response to isolated closed-head injury. *J. Neurosurg.* 66:388–395. <http://dx.doi.org/10.3171/jns.1987.66.3.0388>.
 53. Amthor H, Macharia R, Navarrete R, Schuelke M, Brown SC, Otto A, Voit T, Muntoni F, Vrbóva G, Partridge T, Zammit P, Bunker L, Patel K. 2007. Lack of myostatin results in excessive muscle growth but impaired force generation. *Proc. Natl. Acad. Sci. U. S. A.* 104:1835–1840. <http://dx.doi.org/10.1073/pnas.0604893104>.
 54. Busquets S, Toledo M, Orpi M, Massa D, Porta M, Capdevila E, Padilla N, Frailis V, Lopez-Soriano FJ, Han HQ, Argiles JM. 2012. Myostatin blockage using actRIIB antagonism in mice bearing the Lewis lung carcinoma results in the improvement of muscle wasting and physical performance. *J. Cachexia Sarcopenia Muscle* 3:37–43. <http://dx.doi.org/10.1007/s13539-011-0049-z>.
 55. Akpan I, Goncalves MD, Dhir R, Yin X, Pistilli EE, Bogdanovich S, Khurana TS, Ucran J, Lachey J, Ahima RS. 2009. The effects of a soluble activin type IIB receptor on obesity and insulin sensitivity. *Int. J. Obes. (Lond.)* 33:1265–1273. <http://dx.doi.org/10.1038/ijo.2009.162>.
 56. Fournier B, Murray B, Gutzwiller S, Marcaletti S, Marcellin D, Bergling S, Brachat S, Persohn E, Pierrel E, Bombard F, Hatakeyama S, Trendelenburg AU, Morvan F, Richardson B, Glass DJ, Lach-Trifilieff E, Feige JN. 2012. Blockade of the activin receptor IIB activates functional brown adipogenesis and thermogenesis by inducing mitochondrial oxidative metabolism. *Mol. Cell. Biol.* 32:2871–2879. <http://dx.doi.org/10.1128/MCB.06575-11>.